8th International IFAC Symposium on
Dynamics and Control of Process Systems
Preprints Vol.2, June 6-8, 2007, Cancún, Mexico

HIGHER-ORDER GENERALIZED 2D PREDICTIVE ITERATIVE LEARNING CONTROL SCHEMES

Jia Shi[**], **Furong Gao**[*]

[*]*Department of Chemical Engineering*
Hong Kong University of Science & Technology, Clear Water Bay, Kowloon, Hong Kong
[**]*Department of Automation*
School of Information Science & Technology, Xiamen University, Fujian, 361000, PRC

Abstract: In this paper, based on the prediction control performances defined over one cycle or multiple cycles, two higher-order ILC schemes have been developed by extending the Generalized Predictive Control (GPC) method to the two-dimensional (2D) system. The dynamics of the ILC system along time and cycle is taken as a 2D system, and the proposed designs integrate optimally the design and the combination of a time-wise GPC scheme and a cycle-wise ILC scheme in 2D sense. The simulations show the feasibility and effectiveness of the proposed algorithms.

Keywords: iterative learning control (ILC), Generalized Predictive Control (GPC), two-dimensional (2D) system, inverse dynamic control

1. INTRODUCTION

Iterative learning control (ILC) improves the control performance from cycle to cycle by using the control information of the past cycles. In the earlier researches (Moore, 1993), as the cycle-wise convergence was concerned only, the proposed control laws are essentially open-loop feed-forward control along time for each cycle, which can not guarantee the time-wise control performance within each cycle. To solve this problem, a time-wise feedback control was proposed to combine with cycle-wise ILC, resulting in the *feedback feed-forward ILC* schemes (Amann *et al.*, 1996).

An ILC system is essentially a two-dimensional (2D) system (Kaczorek, 1985), where dynamics along time is determined by process and dynamics along cycle is introduced by ILC law. From 2D system viewpoint, a feedback feed-forward ILC is a 2D feedback control scheme. The major advantage of viewing an ILC system as a 2D system is that the 2D dynamics of the system can be taken into account not only in the process modeling but also in the control performance and controller design, resulting in an united design and optimal combination of the real-time feedback control and cycle-wise ILC in the 2D sense. Since Geng *et al.* (1990) first proposed to describe ILC system as a 2D system, the idea of designing ILC from 2D system viewpoint has attracted considerable interest (Kurek *et al.*, 1993; Yamada *et al.*, 2003; Fang *et al.*, 2003).

It is noted that the most existing ILC laws generate the control input for process from the control information of the last one cycle. In terms of cycle index, this kind of control law is referred as *first-order ILC* law which has relatively poor robust convergence for the uncertainties and disturbance with respect to cycle index. Higher-order ILC laws synthesis the control from the information of past several cycles. It has been illustrated (Bien *et al.*, 1989; Chen *et al.*, 1992) that higher-order ILC scheme has good cycle-wise robustness and convergence.

The objective of this paper is to extend the philosophy of Generalized Predictive Control (GPC) (Clarke *et al.*, 1987) to the 2D system to accommodate the design of the higher-order feedback feed-forward ILC system. The resulted ILC schemes obtained in this paper are, therefore, referred as higher-order *Generalized 2D Predictive Iterative Learning Control (2D-GPILC)*. In consideration of the 2D dynamics of the ILC system, a 2D cost function defined on prediction horizon of current cycle is firstly optimized based on the 2D prediction model of the control system, resulting in a feedback feed-forward ILC scheme referred as single-cycle higher-order 2D-GPILC scheme. The structure analysis indicates that the resulted control scheme consists of a time-wise GPC ensuring the optimal control performances over the time-wise moving prediction horizon and a cycle-wise ILC guaranteeing the control performance improvement along cycle. To enhance the cycle-wise control performance, a multi-cycle predictive cost function is further proposed to optimize, resulting in multi-cycle higher-order 2D-GPILC scheme. The numerical examples are provided to demonstrate the performance of the proposed schemes.

2. PROBLEM FORMULATION

2.1 Process model and higher-order ILC law

For simplicity, it is assumed in this paper that a repetitive process is described by the following SISO CARIMA model

$$\Sigma_P : A(q_t^{-1}) y_k(t) = B(q_t^{-1}) \Delta_t \left(u_k(t)\right) + w_k(t) \quad (1)$$

$$t = 0,1,...,T; \quad k = 1,2,...$$

where t and k represent the discrete-time and cycle index, respectively, T is the time duration of each cycle, $u_k(t)$, $y_k(t)$ and $w_k(t)$ are, respectively, the input, output and unknown disturbance of the process, q_t^{-1} indicates the *time-wise unit backward-shift operator*, $A(q_t^{-1})$ and $B(q_t^{-1})$ are both operator polynomials

$$A(q_t^{-1}) = 1 + a_1 q_t^{-1} + a_2 q_t^{-2} + \cdots + a_n q_t^{-n} \quad (2)$$

$$B(q_t^{-1}) = b_1 q_t^{-1} + b_2 q_t^{-2} + \cdots + b_m q_t^{-m} \quad (3)$$

and Δ_t represents the *time-wise backward difference operator*, i.e. $\Delta_t\left(f_k(t)\right) = f_k(t) - f_k(t-1)$.

For the above process, the following ILC law synthesized from the control information of multiple past cycles, referred as higher-order ILC, is of interest in this paper

$$\Sigma_{ILC} : \Delta_t\left(u_k(t)\right) = \sum_{i=1}^{n_0} \lambda_i \Delta_t\left(u_{k-i}(t)\right) + r_k(t) \quad (4)$$

$$\Delta_t\left(u_i(t)\right) = 0 \text{ for } t = 1,2,...,T, \ i = 0,-1,...,1-n_0$$

where $r_k(t)$ is referred as *updating law* to be determined, $0 \le \lambda_i \le 1, i = 1,2,...,n_0$, satisfying $\sum_{i=1}^{n_0} \lambda_i = 1$, are the specified weighting factors for the control increments of past cycles indicating the contributions of previous controls to the construction of the new control increments. Let q_k^{-1} represent the *cycle-wise unit backward-shift operator*, the transformation between $u_k(t)$ and $r_k(t)$ can be formulated as

$$u_k(t) = \frac{1}{M(q_k^{-1})} \cdot \frac{1}{(1-q_t^{-1})} \cdot r_k(t) \quad (5)$$

where $M(q_k^{-1}) = 1 - \lambda_1 q_k^{-1} - \lambda_2 q_k^{-2} - ... - \lambda_{n_0} q_k^{-n_0}$ is operator polynomial introducing dynamics along cycle index. From 2D system viewpoint, the above control law is a 2D system with a time-wise integrator and cycle-wise filter cascaded in 2D sense. The conventional ILC law (Moore, 1993), commonly formulated as $u_k(t) = u_{k-1}(t) + L\left(e_{k-1}(t)\right)$, however, is only a cycle-wise feedback control with integral action along cycle index. As more past cycle information is used, higher-order ILC law (4) can enhance the robust convergence and disturbance rejection along cycle index.

2.2 Equivalent 2D model and cost function

Substituting (4) into model (1) results in the following closed-loop control system

Σ_{2D-P} :

$$A(q_t^{-1}) y_k(t) = \sum_{i=1}^{n_0} \lambda_i A(q_t^{-1}) y_{k-i}(t) + B(q_t^{-1}) r_k(t) + v_k(t) \quad (6)$$

where $r_k(t)$, $y_k(t)$, $v_k(t) = w_k(t) - \sum_{i=1}^{n_0} \lambda_i w_{k-i}(t)$ are viewed as the input, output and disturbance, respectively. Note that model (6) represents a 2D system where the output of the system depends on both time-wise and cycle-wise historical input-output information. In this paper, model (6) is referred as the *equivalent 2D model* of the ILC system. The design work for updating law $r_k(t)$ is equivalent to design a 2D feedback control law for 2D system (6). For 2D model Σ_{2D-P}, the following quadratic cost function based on the time-wise moving predictive performance over one cycle is defined as the control performance index

$$J(t,k,n_1,n_2) = \sum_{i=1}^{n_1} \eta(i)\left(y_r(t+i) - \hat{y}_{k|k}(t+i\,|\,t)\right)^2 + \sum_{j=0}^{n_2-1} \left(\alpha(j)\left(r_k(t+j)\right)^2 + \beta(j)\left(\Delta_t\left(u_k(t+j)\right)\right)^2\right) \quad (7)$$

where $n_1, n_2 (n_1 \ge n_2)$ are, respectively, referred as the *time-wise prediction horizon* and *time-wise control horizon*, $\hat{y}_{k|k}(t+i\,|\,t)$ indicates the predicted output at i step ahead in the kth cycle based on the measurements before time t of the kth cycle, $y_r(t)$, $t = 0,1,...,T$, is the desired trajectory, $\eta(i) \ge 0$, $\alpha(j) \ge 0$, $\beta(j) \ge 0$, $i = 1,2,...,n_1$, $j = 0,1,...,n_2 - 1$ are the specified weighting factors indicating the importance of each cost terms.

Remark 2.1. In cost function (7), $r_k(t)$, the manipulating variable of 2D system Σ_{2D-P}, is penalized for the improvement of 2D stability and robustness. It is noted from control law (4) that control increment $\Delta_t\left(u_k(t)\right)$ is not independently determined by variable $r_k(t)$. In other word, small value of $r_k(t)$ may also result in significant control increment $\Delta_t\left(u_k(t)\right)$. Excluding $\Delta_t\left(u_k(t)\right)$ in the objective function, optimization will result in a perfect tracking control, i.e. the *inverse dynamic control* for the process, which is hyper-sensitive to high-frequency components of the error and disturbance. Although the penalty of $\Delta_t\left(u_k(t)\right)$ suppresses to a degree the movement of $u_k(t)$ along t, it is helpful to prevent the cycle-wise divergent problem for processes with unstable inverse dynamics. The inclusion of $\Delta_t\left(u_k(t)\right)$ in the cost function can provide a smooth control operation that is important for process control applications.

3. SINGLE-CYCLE HIGHER-ORDER 2D-GPILC

2.3 2D prediction model

In GPC framework, a prediction model for the output estimation over the prediction horizon is required for the derivation of control algorithm. According to 2D equivalent model of the ILC system, at any time t of the k th cycle, the input and output information of the process can be divided into known and unknown parts as follows

$$\begin{pmatrix}\boldsymbol{A}_1 & \boldsymbol{A}_2\end{pmatrix}\begin{pmatrix}\boldsymbol{y}_k\left(|_{t}^{t-n+1}\right)\\ \boldsymbol{y}_k\left(|_{t+n_1}^{t+1}\right)\end{pmatrix}=\begin{pmatrix}\boldsymbol{B}_1 & \boldsymbol{B}_2\end{pmatrix}\begin{pmatrix}\boldsymbol{r}_k\left(|_{t-1}^{t-m+1}\right)\\ \boldsymbol{r}_k\left(|_{t+n_1-1}^{t}\right)\end{pmatrix}+\sum_{i=1}^{n_0}\lambda_i\begin{pmatrix}\boldsymbol{A}_1 & \boldsymbol{A}_2\end{pmatrix}\begin{pmatrix}\boldsymbol{y}_{k-i}\left(|_{t}^{t-n+1}\right)\\ \boldsymbol{y}_{k-i}\left(|_{t+n_1}^{t+1}\right)\end{pmatrix}+\boldsymbol{v}_k\left(|_{t+n_1}^{t+1}\right) \quad (8)$$

where $\boldsymbol{f}_k\left(|_{t_2}^{t_1}\right)=\left(f_k(t_1)\ f_k(t_1+1)\ \cdots f_k(t_2)\right)^T$, $f\in\{y,r,v,u\}$, and

$$\left(\boldsymbol{A}_1\mid\boldsymbol{A}_2\right)=\left(\begin{array}{ccccc|ccccc} a_n & a_{n-1} & a_{n-2} & \cdots & a_1 & 1 & 0 & \cdots & 0 & 0\\ 0 & a_n & a_{n-1} & \cdots & a_2 & a_1 & 1 & \cdots & 0 & 0\\ 0 & 0 & a_n & \cdots & a_3 & a_2 & a_1 & \cdots & 0 & 0\\ \vdots & \vdots & \vdots & \ddots & \vdots & \vdots & \vdots & \ddots & \vdots & \vdots\\ 0 & 0 & 0 & \cdots & * & * & * & \cdots & a_1 & 1\end{array}\right)$$

$$\left(\boldsymbol{B}_1\mid\boldsymbol{B}_2\right)=\left(\begin{array}{ccccc|ccccc} b_m & b_{m-1} & b_{m-2} & \cdots & b_2 & b_1 & 0 & \cdots & 0 & 0\\ 0 & b_m & b_{m-1} & \cdots & b_3 & b_2 & b_1 & \cdots & 0 & 0\\ 0 & 0 & b_m & \cdots & b_4 & b_3 & b_2 & \cdots & 0 & 0\\ \vdots & \vdots & \vdots & \ddots & \vdots & \vdots & \vdots & \ddots & \vdots & \vdots\\ 0 & 0 & 0 & \cdots & * & * & * & \cdots & b_2 & b_1\end{array}\right)$$

As $\boldsymbol{A}_2$ is a nonsingular matrix, it follows from (8) that

$$\boldsymbol{y}_k\left(|_{t+n_1}^{t+1}\right)=\boldsymbol{G}\boldsymbol{r}_k\left(|_{t+n_1-1}^{t}\right)+\sum_{i=1}^{n_0}\lambda_i\boldsymbol{y}_{k-i}\left(|_{t+n_1}^{t+1}\right)+\boldsymbol{F}_k(t)+\boldsymbol{V}_k(t) \quad (9)$$

where

$$\boldsymbol{G}=\boldsymbol{A}_2^{-1}\boldsymbol{B}_2,\quad \boldsymbol{V}_k(t)=\boldsymbol{A}_2^{-1}\boldsymbol{v}_k\left(|_{t+n_1}^{t+1}\right) \quad (10)$$

$$\boldsymbol{F}_k(t)=\boldsymbol{A}_2^{-1}\boldsymbol{B}_1\boldsymbol{r}_k\left(|_{t-1}^{t-m+1}\right)-\boldsymbol{A}_2^{-1}\boldsymbol{A}_1\left(\boldsymbol{y}_k\left(|_{t}^{t-n+1}\right)-\sum_{i=1}^{n_0}\lambda_i\boldsymbol{y}_{k-i}\left(|_{t}^{t-n+1}\right)\right) \quad (11)$$

Clearly, $\boldsymbol{F}_k(t)$ depends on the input-output information of past time over the previous cycles. With assumptions that disturbance $\boldsymbol{v}_k\left(|_{t+n_1}^{t+1}\right)$ is a white noise and $n_1=n_2$, the best prediction of the outputs over the time-wise prediction horizon can be formulated by

$$\hat{\boldsymbol{y}}_{k|k}\left(|_{t+n_1}^{t+1}\mid t\right)=\boldsymbol{G}\boldsymbol{r}_k\left(|_{t+n_1-1}^{t}\right)+\sum_{i=1}^{n_0}\lambda_i\boldsymbol{y}_{k-i}\left(|_{t+n_1}^{t+1}\right)+\boldsymbol{F}_k(t) \quad (12)$$

For $n_1>n_2$ and setting $r_k(t+i)=0$, $i=n_2,\ldots,n_1-1$, the last n_1-n_2 columns of matrix $\boldsymbol{G}$ in the above model should be deleted to accommodate the time-wise control horizon, resulting in a generalized 2D prediction model as follows

$$\hat{\boldsymbol{y}}_{k|k}\left(|_{t+n_1}^{t+1}\mid t\right)=\boldsymbol{G}\boldsymbol{r}_k\left(|_{t+n_2-1}^{t}\right)+\sum_{i=1}^{n_0}\lambda_i\boldsymbol{y}_{k-i}\left(|_{t+n_1}^{t+1}\right)+\boldsymbol{F}_k(t) \quad (13)$$

In the next subsection, higher-order 2D-GPILC algorithm will be developed based on the above prediction model.

2.4 Single-cycle higher-order 2D-GPILC scheme

Quadratic cost function (7) can be expressed in a matrix form

$$J_k(t,n_1,n_2)=\hat{\boldsymbol{X}}_{k|k}^T(t)\bar{\boldsymbol{Q}}\hat{\boldsymbol{X}}_{k|k}(t)+\boldsymbol{r}_k^T(|_{t+n_2-1}^{t})\boldsymbol{R}\boldsymbol{r}_k(|_{t+n_2-1}^{t}) \quad (14)$$

where

$$\hat{\boldsymbol{X}}_{k|k}(t)=\left(\hat{\boldsymbol{e}}_{k|k}^T(|_{t+n_1}^{t+1}\mid t)\quad \Delta_t\left(\boldsymbol{u}_k^T(|_{t+n_2-1}^{t})\right)\right)^T \quad (15)$$

$$\hat{\boldsymbol{e}}_{k|k}(|_{t+n_1}^{t+1}\mid t)=\boldsymbol{y}_r(|_{t+n_1}^{t+1})-\hat{\boldsymbol{y}}_{k|k}(|_{t+n_1}^{t+1}\mid t) \quad (16)$$

$$\boldsymbol{Q}=diag\{\eta(1),\ldots,\eta(n_1)\},\ \boldsymbol{R}=diag\{\alpha(0),\ldots,\alpha(n_2-1)\}$$

$$\boldsymbol{S}=diag\{\beta(0),\ldots,\beta(n_2-1)\},\ \bar{\boldsymbol{Q}}=diag\{\boldsymbol{Q},\boldsymbol{S}\} \quad (17)$$

The above cost function subject to the following 2D prediction model

$$\hat{\boldsymbol{X}}_{k|k}(t)=\bar{\boldsymbol{G}}\boldsymbol{r}_k(|_{t+n_2-1}^{t})+\sum_{i=1}^{n_0}\lambda_i\boldsymbol{X}_{k-i}(t)+\boldsymbol{W}_k(t) \quad (18)$$

where

$$\boldsymbol{e}_{k-1}(|_{t+n_1}^{t+1})=\boldsymbol{y}_r(|_{t+n_1}^{t+1})-\boldsymbol{y}_{k-1}(|_{t+n_1}^{t+1}) \quad (19)$$

$$\boldsymbol{X}_{k-1}(t)=\begin{pmatrix}\boldsymbol{e}_{k-1}(|_{t+n_1}^{t+1})\\ \Delta_t\left(\boldsymbol{u}_{k-1}(|_{t+n_2-1}^{t})\right)\end{pmatrix},\boldsymbol{W}_k(t)=\begin{pmatrix}-\boldsymbol{F}_k(t)\\ \boldsymbol{0}\end{pmatrix},\bar{\boldsymbol{G}}=\begin{pmatrix}-\boldsymbol{G}\\ \boldsymbol{I}\end{pmatrix} \quad (20)$$

It results from optimization algorithm that cost function (14) is minimized by optimal control law $\boldsymbol{r}_k^*(|_{t+n_2-1}^{t})$

$$= -\left(\boldsymbol{R} + \bar{\boldsymbol{G}}^T \bar{\boldsymbol{Q}} \bar{\boldsymbol{G}}\right)^{-1} \bar{\boldsymbol{G}}^T \bar{\boldsymbol{Q}} \left(\sum_{i=1}^{n_0} \lambda_i \boldsymbol{X}_{k-i}(t) + \boldsymbol{W}_k(t) \right) \quad (21)$$

It then follows from (17)(19)(20) that

$$\boldsymbol{r}_k^*(|_{t+n_2-1}^{t}) = \left(\boldsymbol{R} + \boldsymbol{G}^T \boldsymbol{Q} \boldsymbol{G} + \boldsymbol{S}\right)^{-1} \boldsymbol{G}^T \boldsymbol{Q} \left(\sum_{i=1}^{n_0} \lambda_i \boldsymbol{e}_{k-i}(|_{t+n_1}^{t+1}) - \boldsymbol{F}_k(t) \right)$$

$$-\left(\boldsymbol{R} + \boldsymbol{G}^T \boldsymbol{Q} \boldsymbol{G} + \boldsymbol{S}\right)^{-1} \boldsymbol{S} \sum_{i=1}^{n_0} \lambda_i \Delta_t \left(\boldsymbol{u}_{k-i}(|_{t+n_2-1}^{t}) \right) \quad (22)$$

Let $\boldsymbol{K}_1$ and $\boldsymbol{K}_2$ be the first row of matrices $\left(\boldsymbol{R} + \boldsymbol{G}^T \boldsymbol{Q} \boldsymbol{G} + \boldsymbol{S}\right)^{-1} \boldsymbol{G}^T \boldsymbol{Q}$ and $-\left(\boldsymbol{R} + \boldsymbol{G}^T \boldsymbol{Q} \boldsymbol{G} + \boldsymbol{S}\right)^{-1} \boldsymbol{S}$, respectively. In terms of the GPC strategy, the single-cycle higher-order 2D-GPILC algorithm is $\Sigma_{2D-GPILC}$:

$$\Delta_t\left(u_k(t)\right) = \sum_{i=1}^{n_0} \lambda_i \Delta_t\left(u_{k-i}(t)\right) + \boldsymbol{K}_1 \left(\sum_{i=1}^{n_0} \lambda_i \boldsymbol{e}_{k-i}(|_{t+n_1}^{t+1}) - \boldsymbol{F}_k(t) \right)$$

$$+\boldsymbol{K}_2 \sum_{i=1}^{n_0} \lambda_i \Delta_t \left(\boldsymbol{u}_{k-i}(|_{t+n_2-1}^{t}) \right) \quad (23)$$

4. STRUCTURE ANALYSIS

Let $\boldsymbol{K}_1' = \boldsymbol{K}_1$, $\boldsymbol{K}_2' = \boldsymbol{K}_2$, $\boldsymbol{K}_3' = -\boldsymbol{K}_1 \boldsymbol{A}_2^{-1} \boldsymbol{B}_1$, $\boldsymbol{K}_4' = \boldsymbol{K}_1 \boldsymbol{A}_2^{-1} \boldsymbol{A}_1$, it then follows from definition (11) that single-cycle higher-order 2D-GPILC law (23) can be reformulated as

$$r_k(t) = \left(\boldsymbol{K}_1' \quad \boldsymbol{K}_2' \quad \boldsymbol{K}_3' \quad \boldsymbol{K}_4'\right) \begin{pmatrix} \sum_{i=1}^{n_0} \lambda_i \boldsymbol{e}_{k-i}(|_{t+n_1}^{t+1}) \\ \sum_{i=1}^{n_0} \lambda_i \Delta_t \left(\boldsymbol{u}_{k-i}(|_{t+n_2-1}^{t}) \right) \\ \boldsymbol{r}_k\left(|_{t-1}^{t-m+1}\right) \\ \boldsymbol{y}_k\left(|_{t}^{t-n+1}\right) - \sum_{i=1}^{n_0} \lambda_i \boldsymbol{y}_{k-i}\left(|_{t}^{t-n+1}\right) \end{pmatrix}$$

From 2D system viewpoint, the closed-loop system is a 2D feedback control system composed of 2D plant Σ_{2D-P} and 2D feedback controller $\Sigma_{2D-GPILC}$. From ILC system viewpoint, control law (23) can be decomposed as

$$\Sigma_{2D-GPILC}: \Delta_t\left(u_k(t)\right) = u_{ILC,k}(t) + u_{GPC,k}(t) \quad (24)$$

$$\Sigma_{ILC}: u_{ILC,k}(t) = \sum_{i=1}^{n_0} \lambda_i u_{ILC,k-i}(t) + \sum_{i=1}^{n_0} \lambda_i \boldsymbol{K}_1' \boldsymbol{e}_{k-i}\left(|_{t+n_1}^{t+1}\right)$$

$$+\sum_{i=1}^{n_0} \lambda_i \boldsymbol{K}_2' \Delta_t \left(\boldsymbol{u}_{k-i}(|_{t+n_2-1}^{t}) \right) \quad (25)$$

$$\Sigma_{GPC}: u_{GPC,k}(t) = \boldsymbol{K}_3' \Delta_t \left(\boldsymbol{u}_k\left(|_{t-1}^{t-m+1}\right) \right) + \boldsymbol{K}_4' \boldsymbol{y}_k\left(|_{t}^{t-n+1}\right) \quad (26)$$

Obviously, Σ_{ILC} represents a higher-order ILC law using the control errors over the time-wise moving prediction horizon of past n_0 cycles to improve the control performance from cycle to cycle and time-wise control increments over the time-wise moving control horizon of past n_0 cycles to ensure the time-wise robustness and disturbance rejection along time, and Σ_{GPC} is the well-known GPC law based on the real-time feedback information of current cycle to guarantee the control performance along time index. The proposed method designs the two kinds of controls in 2D system framework and results in the optimization of the control performance along time and cycle in 2D sense.

5. MULTI-CYCLE HIGHER-ORDER 2D-GPILC

In consideration of the 2D dynamics of the ILC system, a cost function involving the prediction control performance over multiple cycles is introduced as follows for the further improvement of the control performance along cycle,

$$J_k(t, n_1, n_2, n_3) = \sum_{l=0}^{n_3-1} \gamma(l) \left(\sum_{i=1}^{n_1} \eta(i) \left(\hat{e}_{k+l|k}(t+i \mid t) \right)^2 \right.$$

$$\left. + \sum_{j=0}^{n_2-1} \left(\alpha(j) \left(r_{k+l}(t+j) \right)^2 + \beta(j) \left(\Delta_t\left(u_{k+l}(t+j)\right) \right)^2 \right) \right) \quad (27)$$

where n_3 is referred as the *cycle-wise optimization horizon*, $\hat{e}_{k+l|k}(t+i \mid t) = y_r(t+i) - \hat{y}_{k+l|k}(t+i \mid t)$ represents the estimated control error at time $t+i$ of the $(k+l)$th cycle based on the measurements before time t of the kth cycle, $\gamma(l) > 0$, $l = 0, 1, ..., n_3 - 1$ are the cycle-wise weighting factor, and the definitions of other parameters are the same as cost function (7).

At any time t of the k th cycle, the higher-order 2D-GPILC scheme obtained based on the optimization of cost function (27) is referred as multi-cycle higher-order 2D-GPILC scheme.

To derive the multi-cycle higher-order 2D-GPILC law, the 2D prediction model for the outputs on the cycle-wise optimization horizon, referred as multi-cycle 2D prediction model, is required. It is follows from relationships (4)(9) and definitions (19) (20) that

$$\left(\bar{\boldsymbol{A}}_1 \quad \bar{\boldsymbol{A}}_2\right) \begin{pmatrix} \boldsymbol{X} |_{k-1}^{k-n_0}(t) \\ \boldsymbol{X} |_{k+n_3-1}^{k}(t) \end{pmatrix} = \bar{\boldsymbol{B}} \boldsymbol{r} |_{k+n_3-1}^{k} \left(|_{t+n_2-1}^{t}\right)$$

$$+\left(\bar{\boldsymbol{C}}_1 \quad \bar{\boldsymbol{C}}_2\right) \begin{pmatrix} \boldsymbol{W}_k(t) \\ \boldsymbol{W} |_{k+n_3-1}^{k+1}(t) \end{pmatrix} + \boldsymbol{T} |_{k+n_3-1}^{k}(t) \quad (28)$$

where $\boldsymbol{f} |_{k_2}^{k_1}(t) = \left(\boldsymbol{f}_{k_1}^T(t) \quad \boldsymbol{f}_{k_1+1}^T(t) \quad \cdots \quad \boldsymbol{f}_{k_2}^T(t) \right)^T$, $\boldsymbol{f} \in \{\boldsymbol{X}, \boldsymbol{r}, \boldsymbol{W}, \boldsymbol{T}\}$, and

$\left(\bar{\boldsymbol{A}}_1 \mid \bar{\boldsymbol{A}}_2\right) =$

$$\begin{pmatrix} -\lambda_{n_0}\boldsymbol{I} & -\lambda_{n_0-1}\boldsymbol{I} & -\lambda_{n_0-2}\boldsymbol{I} & \cdots & -\lambda_1\boldsymbol{I} & \boldsymbol{I} & \boldsymbol{0} & \cdots & \boldsymbol{0} & \boldsymbol{0} \\ \boldsymbol{0} & -\lambda_{n_0}\boldsymbol{I} & -\lambda_{n_0-1}\boldsymbol{I} & \cdots & -\lambda_2\boldsymbol{I} & -\lambda_1\boldsymbol{I} & \boldsymbol{I} & \cdots & \boldsymbol{0} & \boldsymbol{0} \\ \boldsymbol{0} & \boldsymbol{0} & -\lambda_{n_0}\boldsymbol{I} & \cdots & -\lambda_3\boldsymbol{I} & -\lambda_2\boldsymbol{I} & -\lambda_1\boldsymbol{I} & \cdots & \boldsymbol{0} & \boldsymbol{0} \\ \vdots & \vdots & \vdots & \ddots & \vdots & \vdots & \vdots & \ddots & \vdots & \vdots \\ \boldsymbol{0} & \boldsymbol{0} & \boldsymbol{0} & \cdots & * & * & * & \cdots & -\lambda_1\boldsymbol{I} & \boldsymbol{I} \end{pmatrix}$$

$$\left(\bar{\boldsymbol{C}}_1 \mid \bar{\boldsymbol{C}}_2\right) = \begin{pmatrix} \boldsymbol{I} & \boldsymbol{0} & \boldsymbol{0} & \cdots & \boldsymbol{0} \\ \boldsymbol{0} & \boldsymbol{I} & \boldsymbol{0} & \cdots & \boldsymbol{0} \\ \boldsymbol{0} & \boldsymbol{0} & \boldsymbol{I} & \cdots & \boldsymbol{0} \\ \vdots & \vdots & \vdots & \ddots & \vdots \\ \boldsymbol{0} & \boldsymbol{0} & \boldsymbol{0} & \cdots & \boldsymbol{I} \end{pmatrix}, \bar{\boldsymbol{B}} = \begin{pmatrix} \bar{\boldsymbol{G}} & \boldsymbol{0} & \cdots & \boldsymbol{0} \\ \boldsymbol{0} & \bar{\boldsymbol{G}} & \cdots & \boldsymbol{0} \\ \vdots & \vdots & \ddots & \vdots \\ \boldsymbol{0} & \boldsymbol{0} & \cdots & \bar{\boldsymbol{G}} \end{pmatrix}$$

$$\boldsymbol{T}_k(t) = \begin{pmatrix} \boldsymbol{V}_k(t) \\ \boldsymbol{0} \end{pmatrix} \quad (29)$$

Note that $\bar{\boldsymbol{A}}_2$ is a non-singular matrix. Together with an assumption that disturbance $\boldsymbol{T}|_{k+n_3-1}^{k}(t)$ is a white noise, a reasonable multi-cycle 2D prediction model is obtained

$$\hat{\boldsymbol{X}}|_{k+n_3-1|k}^{k|k}(t) = \bar{\boldsymbol{A}}_2^{-1}\bar{\boldsymbol{B}}\boldsymbol{r}|_{k+n_3-1}^{k}\left(|_{t+n_2-1}^{t}\right) - \bar{\boldsymbol{A}}_2^{-1}\bar{\boldsymbol{A}}_1\boldsymbol{X}|_{k-1}^{k-n_0}(t) + \bar{\boldsymbol{A}}_2^{-1}\bar{\boldsymbol{C}}_1\boldsymbol{W}_k(t) + \bar{\boldsymbol{A}}_2^{-1}\bar{\boldsymbol{C}}_2\hat{\boldsymbol{W}}|_{k+n_3-1|k}^{k+1|k}(t) \quad (30)$$

where super-vector $\hat{\boldsymbol{X}}|_{k+n_3-1|k}^{k|k}(t)$ and $\hat{\boldsymbol{W}}|_{k+n_3-1|k}^{k+1|k}(t)$ denote respectively the predictions of variables $\boldsymbol{X}|_{k+n_3-1}^{k}(t)$ and $\boldsymbol{W}|_{k+n_3-1}^{k+1}(t)$ at time t in the k th cycle, defined by

$$\hat{\boldsymbol{X}}|_{k+n_3-1|k}^{k|k}(t) = \left(\hat{\boldsymbol{X}}_{k|k}^{T}(t) \quad \hat{\boldsymbol{X}}_{k+1|k}^{T}(t) \quad \cdots \quad \hat{\boldsymbol{X}}_{k+n_3-1|k}^{T}(t)\right)^{T} \quad (31)$$

$$\hat{\boldsymbol{W}}|_{k+n_3-1|k}^{k+1|k}(t) = \left(\hat{\boldsymbol{W}}_{k+1|k}^{T}(t) \quad \hat{\boldsymbol{W}}_{k+2|k}^{T}(t) \quad \cdots \quad \hat{\boldsymbol{W}}_{k+n_3-1|k}^{T}(t)\right)^{T} \quad (32)$$

However, as $\hat{\boldsymbol{W}}|_{k+n_3-1|k}^{k+1|k}(t)$ is a prediction variable, the control law obtained based on the above prediction model will be non-causal. If it is assumed that $\boldsymbol{r}_{k+i}\left(|_{t-1}^{1}\right) \equiv \boldsymbol{0}, i = 1,2,...,n_0$, then, from (1)(4)(11)(20), one has $\hat{\boldsymbol{W}}|_{k+n_3-1|k}^{k+1|k}(t) = \boldsymbol{0}$, leading to the following simplified prediction model obtained

$$\hat{\boldsymbol{X}}|_{k+n_3-1}^{k}(t) = \tilde{\boldsymbol{G}}\boldsymbol{r}|_{k+n_3-1}^{k}\left(|_{t+n_2-1}^{t}\right) + \tilde{\boldsymbol{F}}_k(t) \quad (33)$$

where $\tilde{\boldsymbol{G}} = \bar{\boldsymbol{A}}_2^{-1}\bar{\boldsymbol{B}}$ and $\tilde{\boldsymbol{F}}_k(t) = -\bar{\boldsymbol{A}}_2^{-1}\bar{\boldsymbol{A}}_1\boldsymbol{X}|_{k-1}^{k-n_0}(t) + \bar{\boldsymbol{A}}_2^{-1}\bar{\boldsymbol{C}}_1\boldsymbol{W}_k(t)$ which is a vector depends on the input-output information of past n_0 cycles.

It follows from definitions (16)-(17) that cost function (27) can be reformed as

$$J(t,k,n_1,n_2,n_3) = \hat{\boldsymbol{X}}|_{k+n_3-1|k}^{k|k\;T}(t)\tilde{\boldsymbol{Q}}\hat{\boldsymbol{X}}|_{k+n_3-1|k}^{k|k}(t) + \boldsymbol{r}|_{k+n_3-1}^{k\;T}(|_{t+n_2-1}^{t})\tilde{\boldsymbol{R}}\boldsymbol{r}|_{k+n_3-1}^{k}(|_{t+n_2-1}^{t}) \quad (34)$$

where

$$\tilde{\boldsymbol{Q}} = diag\{\gamma(0)\bar{\boldsymbol{Q}}, \gamma(1)\bar{\boldsymbol{Q}}, ..., \gamma(n_3-1)\bar{\boldsymbol{Q}}\} \quad (35)$$

$$\tilde{\boldsymbol{R}} = diag\{\gamma(0)\boldsymbol{R}, \gamma(1)\boldsymbol{R}, ..., \gamma(n_3-1)\boldsymbol{R}\} \quad (36)$$

It again follows from the optimization algorithm that the above cost function is minimized by the following optimal control

$$\boldsymbol{r}|_{k+n_3-1}^{k\;*}\left(|_{t+n_2-1}^{t}\right) = -\left(\tilde{\boldsymbol{R}} + \tilde{\boldsymbol{G}}^{T}\tilde{\boldsymbol{Q}}\tilde{\boldsymbol{G}}\right)^{-1}\tilde{\boldsymbol{G}}^{T}\tilde{\boldsymbol{Q}}\tilde{\boldsymbol{F}}_k(t) \quad (37)$$

In terms of GPC strategy, only the first element of $\boldsymbol{r}|_{k+n_3-1}^{k\;*}\left(|_{t+n_2-1}^{t}\right)$ is applied to the process at each time.

6. EXAMPLE

To illustrate the effectiveness and feasibility of the proposed ILC schemes, it is assumed that the real repetitive process is described by the following model with unknown parameter perturbation and disturbance

$$y_k(t) = \frac{2.651(\pm 2\%)q_t^{-1} + 5.298(\pm 2\%)q_t^{-2} + 0.5805(\pm 2\%)q_t^{-3}}{1 - 1.454(\pm 2\%)q_t^{-1} + 0.5285(\pm 2\%)q_t^{-2} - 0.04736(\pm 2\%)q_t^{-3}} \bullet u_k(t) + v_k(t), \quad t = 0,1,...,200 \quad (38)$$

where the bracketed numbers indicate the boundaries of the uncertain parameter perturbations around the nominal values, which are set in random variables with respect to the cycle index in the following simulations, and $v_k(t)$ represents the effect of the unmodelled dynamics, disturbance and measurement noise of the process, defined by

$$v_k(t) = 20\sin(0.02\pi t) + 0.2n_k(t) \quad (39)$$

where $n_k(t)$ is a random noise uniformly distributed over $[-1,1]$. Clearly, the first term in right-hand-side is cycle-independent, simulating a nonlinear repeatable disturbance, while the second term represents a non-repeatable disturbance, such as measurement noise.

For controller design, the following simplified model is obtained by identification algorithm

$$y_k(t) = \frac{13.81q_t^{-1}}{1 - 0.9524q_t^{-1}}q_t^{-1}u_k(t) \quad (40)$$

Note from (38) and (40) the model-plant -mismatch is significant.

Table 1. Design parameters

Single-cycle high-order 2D-GPILC scheme	***Multi-cycle high-order 2D-GPILC scheme***
$n_0 = 3,\ n_1 = 15,\ n_2 = 10$	$n_0 = 3,\ n_1 = 15,\ n_2 = 10$
$\lambda_i = 1/3,\ \eta = 1,\ \alpha$=2000	$n_3 = 3, \lambda_i = 1/3,\ \eta = 1$
β=5	α=2000, β=5

The design parameters for the proposed higher-order 2D-GPILC schemes are given in Table 1. The system responses and control inputs for the sing-cycle and multi-cycle higher-order 2D-GPILC schemes are shown in Fig. 1 and Fig. 2, respectively, which illustrate the effectiveness and performances of the proposed two ILC schemes. Although, for the multi-cycle scheme, the cycle-wise zero initial condition for ILC law (4) results in significant control error in the first cycle, it is found form the comparison of the sum of squire error (SSE) over each cycle, as shown in Fig. 3, that multi-cycle higher-order 2D-GPILC scheme has faster convergence rate along cycle index.

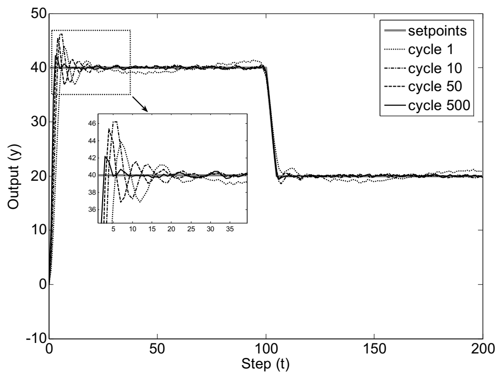

Fig. 1. Output responses of single-cycle higher-order 2D-GPILC scheme.

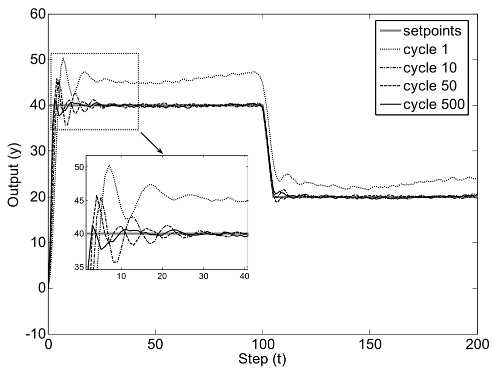

Fig. 2. Output responses of multi-cycle higher-order 2D-GPILC scheme

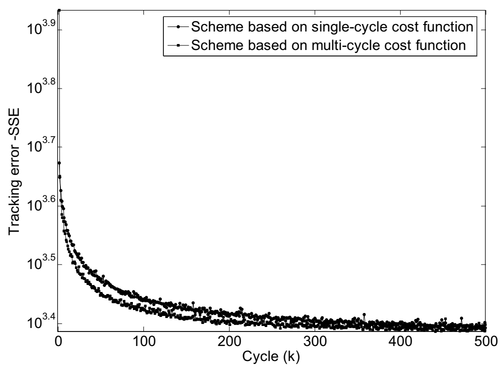

Fig. 3. Comparison of cycle-wise control performances using single-cycle and multi-cycle higher-order 2D-GPILC schemes.

7. CONCLUSIONS

In this paper, the philosophy of GPC has been extended to the 2D system to solve the design problem of higher-order ILC. Based on the prediction performance indices defined over single cycle and multiply cycles, single-cycle and multi-cycle higher-order 2D-GPILC schemes have been developed. The proposed design methods guarantee the integrated design and optimal combination of a time-wise GPC scheme and cycle-wise ILC scheme in 2D sense.

REFERENCES

Amann, N., D.H. Owens and E. Rogers (1996). Iterative learning control using feedback and feedforward actions. *International Journal of Control*, **65**, 277-293.

Bien, Z. and K.M. Huh (1989). Higher-order iterative learning control algorithm. *IEE Proceeding -D: Control Theory and Applications*, **136**, 105-112.

Chen, Y., M. Sun, B. Huang and H. Dou (1992). Robust higher order repeaitive learning control algorithm for tracking control of delayed repetitive systems. In: *Proceeding of the 31st Conference on Decision and Control*. pp. 2504-2510. Tucson, Artzona.

Clarke, D.W., C. Mohtadi and P.S. Tuffs (1987). Generalized Predictive Control--Part I: The Basic Algorithm. *Automatica*, **23**, 137-148.

Fang, Y., T.W.S. Chow (2003). 2-D analysis for iterative learning controller for discrete-time systems with variable initial conditions. *IEEE Transactions on Circuits and Systems-I: Fundamental Theory and Applications*, **50**, 722-727.

Geng, Z., R. Carroll and J. Xie (1990). Two-dimensional model and algorithm analysis for a class of iterative learning control systems. *International Journal of Control*, **52**, 833-862.

Kaczorek, T. (1985). *Two-dimensional linear system*. Springer, Berlin.

Kurek, J.E. and M.B. Zaremba (1993). Iterative learning control synthesis on 2-D system theory. *IEEE Transactions on automatic control*, **38**, 121-125.

Moore, K.L. (1993). *Iterative learning control for deterministic systems*. Springer, London.

Yamada, M., L. Xu and O. Saito (2003). Iterative control of three link manipulator using 2D system control approach. In: *Proceeding of the SICE Annual Conference*, pp. 1880-1885. Fukui University, Japan.